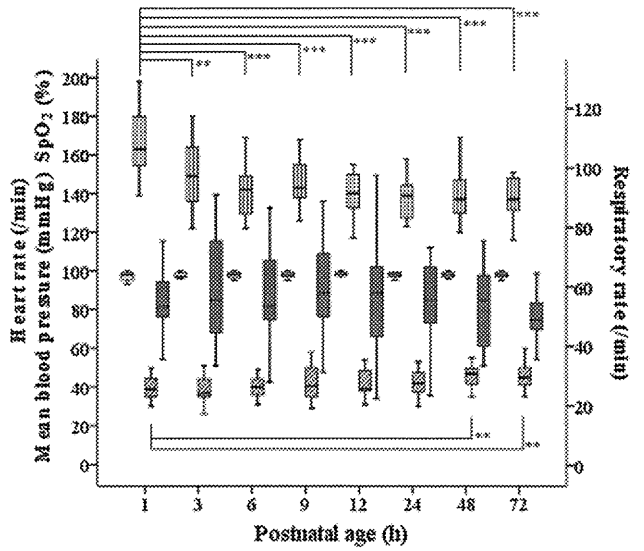

Fig. 3 Changes in heart rate, mean blood pressure, respiratory rate, and SpO_2. The *box* shows the median (*central line*) with interquartile range (25–75th percentile) and the *whisker* represents the 5–95th percentile. *Vertically filled square* heart rate, *diagonally filled square* mean blood pressure, *fully filled square* respiratory rate, *empty filled square* SpO_2. $^{**}p < 0.01$, $^{***}p < 0.001$

Changes in standard echocardiographic measurements (Table 2)

Echocardiography was performed at 1.0 [0.9–1.2] h, 3.0 [3.0–3.2] h, 6.0 [6.0–6.1] h, 9.0 [9.0–9.5] h, 12.0 [11.9–12.3] h, 24.3 [24.0–25.8] h, 48.4 [47.6–49.7] h, and 72.0 [71.5–78.0] h after birth. The LA/Ao ratio decreased significantly from 1.5 ± 0.3 at 1 h to 1.2 ± 0.2 at 9 h ($p = 0.028$), 1.3 ± 0.2 at 24 h ($p = 0.049$), and 1.1 ± 0.2 at 48 h ($p = 0.001$). RVFAC increased from 38.5 ± 9.8 at 1 h to 42.1 ± 8.9 at 48 h ($p = 0.017$), and 47.7 ± 3.6 at 72 h ($p = 0.002$). The AcT/RVET ratio increased significantly from 0.21 ± 0.05 at 1 h to 0.33 ± 0.09 at 24 h ($p = 0.005$), 0.35 ± 0.10 at 48 h ($p < 0.001$), and 0.31 ± 0.10 at 72 h ($p = 0.002$). The LVDd, LVSF and TAPSE did not change during the 72 h after birth. Tissue Doppler-derived MPI at the three measurement points did not change during the study period.

Changes in 2D speckle-tracking strain measurements (Table 2 and Fig. 4)

The bright line was visible in the middle of the VS in the four-chamber view in all subjects. The peak LS on the right side and the left side of the VS and RV free wall did not change during the 72 h after birth. The peak LS was significantly larger on the left side of the VS than on the right side of the VS at 1 h (−22.7 ± 5.7 vs −17.9 ± 4.5 %, $p = 0.047$), 48 h (−19.8 ± 3.1 vs −17.3 ± 4.5 %, $p = 0.048$), and 72 h (−20.9 ± 3.0 vs −14.7 ± 4.6 %, $p = 0.002$). The peak LS remained significantly larger on the RV free wall than on the right side of the VS throughout the study period ($p < 0.01$). The global LV peak LS did not change during the first 72 h of life.

Feasibility and reproducibility of 2D speckle-tracking strain measurements (Table 3)

Strain measurement was feasible in the majority of acquired images—141/150 images (94 %) of the VS, 118/137 images (86 %) of the RV free wall, and 132/144 images (92 %) of the LV. The feasibility of images of the VS was significantly higher compared to that of the RV free wall ($p = 0.01$). For intra-observer reproducibility, Bland–Altman analysis showed minimal bias (<10 %), and the ICC showed moderate to substantial agreement in four strain measurement sites (0.560–0.744). For inter-observer reproducibility, Bland–Altman analysis showed minimal bias (<10 %), and the ICC showed substantial agreement in three speckle-tracking strain measurement sites (0.717–0.758), except the RV free wall, in which the ICC showed modest agreement of 0.455.

Changes in the ductus arteriosus and foramen ovale over time

PDA was seen in 21 infants at 1 h, 18 infants at 3 h, 17 infants at 6 h, 14 infants at 9 h, 13 infants at 12 h, 7 infants at 24 h, 3 infants at 48 h, and 1 infant at 72 h. Compared with 1 h, cases of patency were significantly decreased at 12 h ($p = 0.033$), 24 h ($p < 0.001$), 48 h ($p < 0.001$), and 72 h ($p < 0.001$). Symptomatic PDA was not seen in any case. The left to right shunt through the foramen ovale was observed constantly in all infants during the study period.

Analysis of factors affecting echocardiographic measurements and correlations of regional strain values (Tables 4, 5)

On multiple regression analysis, LVDd and TAPSE appeared significantly associated with birth weight. LVDd was associated with PDA at 12 h and use of n-DPAP at 48 h. Peak LS on the right and left side of the VS was significantly associated with use of n-DPAP in an opposite direction. The associations between peak LS and oxygen administration were inconsistent between the right side of the VS and the RV free wall. The RV free wall peak LS and the global LV peak LS were significantly associated with MPI lateral tricuspid and MPI septal mitral, respectively. The peak LS on the right side of the VS was associated with TAPSE, and the RV free wall peak LS was associated with AcT/RVET. Correlation analysis showed a significant correlation between peak LS on the right side

Table 2 Echocardiographic data during the first 72 h of life

Postnatal age (h)	1	3	6	9
LVDd (cm)	1.6 ± 0.2	1.6 ± 0.2	1.6 ± 0.3	1.5 ± 0.2
LVSF (%)	32.0 [25.3–38.0]	28.0 [26.4–38.8]	28.5 [22.3–36.7]	28.7 [24.0–32.8]
LA/Ao	1.5 ± 0.3	1.3 ± 0.2	1.2 ± 0.3	1.2 ± 0.2*
TAPSE (cm)	0.73 ± 0.10	0.69 ± 0.10	0.71 ± 0.07	0.66 ± 0.07
RVFAC (%)	38.5 ± 9.8	41.4 ± 6.3	31.9 ± 6.9	38.4 ± 8.5
AcT/RVET	0.21 ± 0.05	0.22 ± 0.04	0.27 ± 0.06	0.27 ± 0.09
MPI lateral tricuspid	0.47 ± 0.10	0.44 ± 0.10	0.47 ± 0.06	0.49 ± 0.08
MPI septal mitral	0.54 [0.45–0.70]	0.48 [0.39–0.56]	0.62 [0.57–0.67]	0.54 [0.50–0.58]
MPI lateral mitral	0.46 [0.42–0.54]	0.51 [0.50–0.57]	0.51 [0.40–0.60]	0.51 [0.43–0.61]
VSR peak LS (%)	−17.9 ± 4.5†	−16.2 ± 4.3	−14.6 ± 4.6	−16.3 ± 4.0
VSL peak LS (%)	−22.7 ± 5.7	−17.6 ± 3.4	−16.5 ± 3.9	−19.0 ± 6.9
RVFW peak LS (%)	−22.0 ± 4.7‡	−21.9 ± 5.8‡	−19.3 ± 3.6‡	−22.4 ± 3.0‡
GLV peak LS (%)	−23.8 ± 4.0	−24.2 ± 4.1	−20.4 ± 6.2	−23.0 ± 2.0
Postnatal age (h)	12	24	48	72
LVDd (cm)	1.6 ± 0.2	1.5 ± 0.2	1.5 ± 0.1	1.5 ± 0.3
LVSF (%)	26.9 [25.6–30.8]	31.5 [26.9–37.2]	25.7 [22.8–31.3]	30.0 [28.6–31.5]
LA/Ao	1.2 ± 0.2	1.3 ± 0.2*	1.1 ± 0.2**	1.2 ± 0.3
TAPSE (cm)	0.75 ± 0.09	0.76 ± 0.07	0.70 ± 0.06	0.74 ± 0.10
RVFAC (%)	43.4 ± 5.9	41.5 ± 9.3	42.1 ± 8.9*	47.7 ± 3.6**
AcT/RVET	0.27 ± 0.07	0.33 ± 0.09**	0.35 ± 0.10***	0.31 ± 0.10**
MPI lateral tricuspid	0.44 ± 0.06	0.40 ± 0.12	0.46 ± 0.13	0.41 ± 0.07
MPI septal mitral	0.50 [0.42–0.59]	0.46 [0.38–0.53]	0.43 [0.38–0.53]	0.49 [0.48–0.56]
MPI lateral mitral	0.45 [0.40–0.55]	0.47 [0.41–0.49]	0.54 [0.50–0.60]	0.47 [0.40–0.56]
VSR peak LS (%)	−18.8 ± 3.9	−17.7 ± 4.6	−17.3 ± 4.5†	−14.7 ± 4.6††
VSL peak LS (%)	−22.5 ± 5.4	−21.0 ± 5.1	−19.8 ± 3.1	−20.9 ± 3.0
RVFW peak LS (%)	−21.7 ± 5.0‡	−24.7 ± 4.7‡	−20.8 ± 2.6‡	−22.9 ± 5.1‡
GLV peak LS (%)	−24.9 ± 3.1	−23.4 ± 3.2	−23.8 ± 5.1	−24.9 ± 3.2

Data are presented as mean ± standard deviation or medians (inter-quartile range)

LVDd left ventricular end-diastolic dimension, *LVSF* left ventricular shortening fraction, *LA/Ao* left atrial/aortic root ratio, *TAPSE* tricuspid annular plane systolic excursion, *RVFAC* right ventricular fractional area change, *AcT/RVET* acceleration time/right ventricular ejection time ratio, *MPI* myocardial performance index, *VSR* right side of ventricular septum, *VSL* left side of ventricular septum, *RVFW* right ventricular free wall, *GLV* global left ventricle, *LS* longitudinal strain

* $p < 0.05$, ** $p < 0.01$, *** $p < 0.001$ compared with 1 h after birth

† VSR peak LS compared with VSL peak LS, $p < 0.05$

†† VSR peak LS compared with VSL peak LS, $p < 0.01$

‡ VSR peak LS compared with RVFW peak LS, $p < 0.01$

VS and on the RV free wall at 72 h ($r = 0.593$, $p < 0.001$), and peak LS on the left side of the VS and on the global LV at 72 h ($r = 0.55$, $p = 0.007$).

Discussion

In the present study, peak LS was maintained at the four analyzed regions during the first 72 h of life despite significant hemodynamic changes, including decreased heart rate and increased mean blood pressure, and decreased pulmonary artery pressure and PDA closure as assessed by conventional echocardiography. The peak LS was significantly larger on the left side of the VS than on the right side of the VS at 1, 48, and 72 h after birth. To the best of our knowledge, this is the first report of serial measurement of systolic LS on both sides of the VS, RV, and LV in preterm infants using 2D speckle-tracking echocardiography.

There are few studies of 2D speckle-tracking echocardiography examining fetal or neonatal myocardial

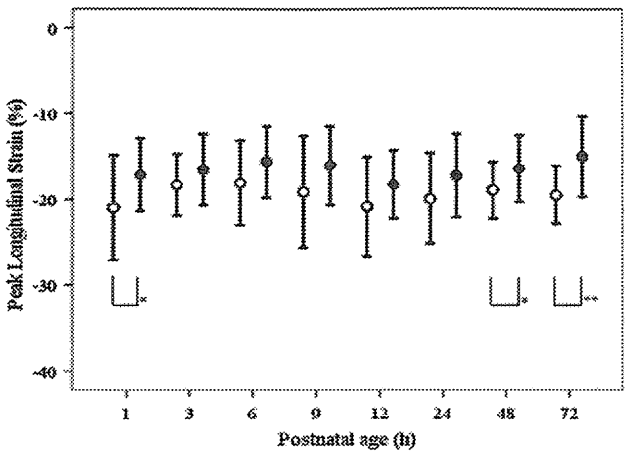

Fig. 4 Changes in 2D speckle-tracking strain measurements on the *right side* and the *left side* of the ventricular septum. The peak longitudinal strain is significantly larger on the *left side* than on the *right side* of the ventricular septum at 1, 48, and 72 h after birth. The *bar* shows the mean ± standard deviation. *Fully filled circle*, *right side* of the ventricular septum; *empty filled circle*, *left side* of the ventricular septum. $*p < 0.05$, $**p < 0.01$

performance. In normal fetuses, Di Salvo et al. [8] studied LS in RV, VS and LV during 20–32 weeks of gestation and found significant correlations between gestational age and LS ($n = 100$). In healthy term infants, Schubert et al. [9] found that LS values at a mean 170 (range 135–207) h after birth were significantly larger in the RV than in the LV and VS ($n = 30$). These values were significantly decreased compared to fetal values of the same infants at 28 weeks of gestation. Jain et al. [10] reported that RV free wall LS was maintained between 15 ± 2 h and 35 ± 2 h of age in healthy term newborns ($n = 50$). In preterm infants, Levy et al. [11] reported high feasibility and reproducibility of RV LS measurement in 50 infants with 27 ± 1 gestational weeks and 0.96 ± 0.2 kg birth weight at 32 weeks (1.42 ± 0.3 kg body weight) and at 36 weeks postmenstrual age (2.21 ± 0.3 kg body weight), but exact values and comparisons between LS measurements at two time points were not included. Using tissue Doppler imaging, it has been found that LS of the VS, RV, and LV did not change between 10 and 45 h post-delivery in 54 preterm infants with a median gestation and birth weight of 26.5 weeks and 915 g, respectively. All infants in this study received early surfactant prior to the first echocardiography, 61 % received mechanical ventilation, and all infants had large unconstricted PDA at 10 h of age [4]. The results of the present study and those of previous studies [4, 9, 10] might indicate that abrupt changes in LS occur at the time of cord clumping and removal of the placenta and that LS is maintained at the VS, RV, and LV to some extent despite significant hemodynamic changes during the transition period in preterm infants. This study reveals that the peak LS of the VS, RV, and LV is relatively independent of hemodynamic changes and can therefore serve as an index for myocardial evaluation during the transition in preterm infants.

Longitudinal deformation was significantly larger on the left side of the VS than on the right side of the VS at 1, 48, and 72 h after birth. This is contrary to previous findings from normal subjects [5, 7]. Boettler et al. [5] found similar LS on the right and on the left VS in healthy adults ($n = 30$, age range 18–53 years) using Doppler myocardial imaging. Hayabuchi et al. [7] reported similar findings in normal children ($n = 132$, age range 1.0–10.0 years) using 2D speckle-tracking echocardiography. They speculated

Table 3 Intra-observer and inter-observer variabilities

	1st Mean ± SD	2nd Mean ± SD	*p* value	Bias (95 % LOA)	ICC
Intra-observer variability					
VSR peak LS (%)	−18.5 ± 4.2	−18.3 ± 4.3	0.919	0.2 (−7.9 to 8.3)	0.560
VSL peak LS (%)	−20.9 ± 4.4	−20.0 ± 3.8	0.628	0.9 (−4.9 to 6.7)	0.744
RVFW peak LS (%)	−23.3 ± 3.6	−21.9 ± 3.6	0.389	1.4 (−4.3 to 7.1)	0.628
GLV peak LS (%)	−26.0 ± 2.2	−24.7 ± 2.8	0.263	1.3 (−1.5 to 4.0)	0.739
	Observer 1 Mean ± SD	Observer 2 Mean ± SD	*p* value	Bias (95 % LOA)	ICC
Inter-observer variability					
VSR peak LS (%)	−18.3 ± 4.3	−17.4 ± 3.1	0.576	1.0 (−4.1 to 6.0)	0.758
VSL peak LS (%)	−20.0 ± 3.8	−20.4 ± 3.0	0.814	−0.4 (−5.6 to 4.9)	0.717
RVFW peak LS (%)	−21.9 ± 3.6	−21.0 ± 4.5	0.604	1.0 (−7.5 to 9.4)	0.455
GLV peak LS (%)	−24.7 ± 2.8	−25.2 ± 3.7	0.736	−0.5 (−4.9 to 4.0)	0.717

VSR right side of ventricular septum, *VSL* left side of ventricular septum, *RVFW* right ventricular free wall, *GLV* global left ventricle, *LS* longitudinal strain, *LOA* limits of agreement, *ICC* intraclass correlation coefficient

Table 4 Clinical factors affecting echocardiographic measurements

Postnatal age (h)	Dependent variable	Independent variable	β	p	R^2
1	TAPSE	Birth weight	0.921	<0.001	0.734
6	GLV peak LS	Use of n-DPAP	0.59	0.002	0.630
	RVFW peak LS	O_2 administration	0.729	0.002	0.495
12	LVDd	Birth weight	0.636	0.001	0.534
		PDA	0.495	0.005	0.534
48	LVDd	Use of n-DPAP	−0.525	0.004	0.536
	VSR peak LS	Use of n-DPAP	−0.498	0.018	0.514
		O_2 administration	−0.728	0.002	0.514
72	LVDd	Birth weight	0.769	<0.001	0.568
	VSL peak LS	Use of n-DPAP	0.616	0.014	0.325

β standardized coefficient, R^2 coefficient of determination, *TAPSE* tricuspid annular plane systolic excursion, *RVFW* right ventricular free wall, *VSR* right side of ventricular septum, *VSL* left side of ventricular septum, *LVG* global left ventricle, *LS* longitudinal strain, *n-DPAP* nasal directional positive airway pressure, *PDA* patent ductus arteriosus

Table 5 Conventional echocardiographic measurements affecting speckle-tracking echocardiographic measurements

Postnatal age (h)	Dependent variable	Independent variable	β	p	R^2
1	GLV peak LS	MPI septal mitral	1.017	<0.001	0.827
	VSR peak LS	TAPSE	−0.749	0.002	0.525
	RVFW peak LS	MPI lateral tricuspid	0.583	0.029	0.285
6	GLV peak LS	MPI septal mitral	0.498	0.047	0.378
12	RVFW peak LS	AcT/RVET	0.534	0.033	0.235

β standardized coefficient, R^2 coefficient of determination, *GLV* global left ventricle, *VSR* right side of ventricular septum, *RVFW* right ventricular free wall, *LS* longitudinal strain, *MPI* myocardial performance index, *TAPSE* tricuspid annular plane systolic excursion, *AcT/RVET* acceleration time/right ventricular ejection time ratio

that the close connection of both sides of the VS prevented independent longitudinal movement, and each side affected the other. Interestingly, however, Hayabuchi et al. [6] documented in another report that in patients ($n = 22$, age 9.0 ± 4.2 years) with a hemodynamically significant atrial septal defect, LS on both sides of the VS was significantly larger than in controls. Furthermore, LS on the left side of the VS was significantly larger than on the right side of the VS.

A geometric model showed that the right and left sides of the VS respond differently to various conditions [21]. At birth, the systemic vascular resistance abruptly increases with discontinuation of the low-resistance placental circulation. Data for right ventricular preload are less conclusive, but it seems that preload drops with clamping of the umbilical cord and rises within hours to supra-fetal levels [9]. The rapid decrease in pulmonary vascular resistance and the increase in pulmonary blood flow augments preload to the left side of the heart. The increased ductal left-to-right shunt also enhances venous return to the left atrium, which will raise left atrial pressure. If the foramen ovale is patent, an atrial left-to-right shunt may raise right ventricular output to levels above those of systemic venous return [14, 22]. All subjects in the present study had a patent foramen ovale until 72 h of age. Although the magnitude of the shunt was not quantified, both ductal and atrial shunts might have caused a significant right ventricular volume overload and affected LS of the VS along with left ventricular pressure and volume overload. It is also plausible that inotropic stimulation with the catecholamine surge induced by delivery affects strain measurements immediately after birth. During the following days, the loading conditions of the right and left ventricles further changed along with a further decrease in pulmonary vascular resistance and closure of the ductal shunt. All these responses might have altered the myocardial performance of the RV and LV and affected the longitudinal deformation of the VS. The different deformation between the bilayered VS might indicate the presence of the delicate pressure and volume adaptation, which is not shown on the RV free wall and global LV deformation.

The peak LS on the right and left sides of the VS was significantly associated with use of n-DPAP at 48 and 72 h, respectively, in an opposite direction. The global LV peak LS and LVDd were also significantly associated with use of n-DPAP at 6 and 48 h, respectively. To our knowledge,

the impact of n-DPAP on myocardial deformation in preterm infants was not addressed previously. In adult patients with obstructive sleep apnea, a few studies demonstrated that chronic therapy using n-DPAP improved both right and left ventricular LS [23, 24]. However, the mechanisms by which n-DPAP alter the hemodynamic status of patients are complex. It has been shown that incremental positive end-expiratory pressure affects the right and left ventricular LS differently and results in a change in right and left ventricular dimensions inversely in adult patients [25]. Since there were significant correlations between LS on the right side of the VS and the RV free wall and between LS on the left side of the VS and global LV at 72 h after birth, the present results suggest that the right and left sides of the VS respond differently to the multiple and complex cardiopulmonary transitions from fetal to neonatal life in preterm infants and that peak LS on the right and left sides of VS might be a sensitive parameter to detect subtle changes in regional myocardial performance in patients with n-DPAP.

The feasibility and reproducibility of 2D strain measurement in the present study were in agreement with previous studies [6–11, 26], but feasibility was lower for the RV free wall than for the VS. For inter-observer reproducibility, the ICC showed substantial agreement on both sides of the VS and the LV, whereas the ICC for the RV free wall was modest. These results might be related to the method of image acquisition of the RV; a standard apical four-chamber view was used in order to avoid interfering with respiration of small infants. The RV myofiber architecture is characterized by dominant longitudinal layers aligned from the base to apex, which allow greater longitudinal than radial shortening and twisting and rotational movements [10]. It is important to define the full extent of the RV free wall to avoid the loss of the optimum number of RV segments through the cardiac cycle for tracking the longitudinal movement [10, 27]. The standard apical four-chamber view might have failed to include the entire RV free wall in its imaging plane and led to poor speckle-tracking. Recently, an RV-focused view has been advocated for high clinical feasibility and reproducibility [10, 15].

Study limitations

Several study limitations should be addressed. First, this study included a small number of infants in a single center, and a larger study is needed to determine the myocardial response during the transitional period in preterm infants. Second, a standard apical four-chamber view was used and not a RV-focused view or any other view, which might have affected LS measurements of the RV free wall. Third, the focus was on mid-ventricular regions of the VS and RV free wall. The myofibers in the base and mid regions of the VS have longitudinal orientation, and the fibers of its apex have circumferential orientation, according to Torrent-Guasp et al. [28]. A recent meta-analysis showed a significant base to apex segmental strain gradient in the RV free wall in normal children [29]. Comparisons with strain values from different regions are necessary to determine the global myocardial performance in preterm infants. Fourth, in this study, we measured the LS and analyzed its correlation with clinical and conventional echocardiographic characteristics. However, the circumferential strain of both sides of VS might have the different pattern in this period. Hayabuchi et al. [6] reported that the longitudinal deformation of both sides of VS was similar in normal children, whereas circumferential strain was significantly different. Finally, a commercially available ultrasound system and vendor-customized software, which are different from those used in most previous pediatric studies, were used [8–10]. Since strain measurements are reported to be significantly different for each of the vendors [30], care should be taken when comparing results between studies.

Conclusion

Preterm infants without mechanical ventilation, inotropic agents, or symptomatic PDA showed stable LS on both sides of the VS, RV free wall, and LV despite hemodynamically significant changes during the first 72 h of life. LS was significantly larger on the left side of the VS than on the right side of the VS at 1, 48, and 72 h after birth, and the responsible mechanisms and clinical implications should be elucidated in further studies.

Acknowledgment This study was approved by the institutional review board of Iwate Medical University (H25-63).

Conflict of interest Yurie Nasu, Kotaro Oyama, Satoshi Nakano, Atsushi Matsumoto, Wataru Soda, Shin Takahashi, and Shoichi Chida declare that they have no conflict of interest.

Human rights statement and informed consent All procedures followed were in accordance with the ethical standards of the institutional review board of Iwate Medical University and with the Helsinki Declaration of 1975, as revised in 2000. Informed consent was obtained from the parents of all subjects prior to enrolment.

References

1. Kluckow M, Seri I. Clinical presentations of neonatal shock: the very low birth weight neonate during the first postnatal day. In: Kleinman CS, Seri I, Polin RA editors. Hemodynamics and Cardiology. Neonatology Questions and Controversies. 2nd ed. Philadelphia, Elsevier Saunders; 2012. pp. 237-67.

2. El-Khuffash AF, Jain A, Dragulescu A, et al. Acute changes in myocardial systolic function in preterm infants undergoing patent ductus arteriosus ligation: a tissue Doppler and myocardial deformation study. J Am Soc Echocardiogr. 2012;25:1058–67.
3. Lee A, Nestaas E, Liestol K, et al. Tissue Doppler imaging in very preterm infants during the first 24 h of life: an observational study. Arch Dis Child Fetal Neonatal Ed. 2014;99:F64–9.
4. James AT, Corcoran JD, Jain A, et al. Assessment of myocardial performance in preterm infants less than 29 weeks gestation during the transitional period. Early Hum Dev. 2014;90:829–35.
5. Boettler P, Claus P, Herbots L, et al. New aspects of the ventricular septum and its function: an echocardiographic study. Heart. 2005;91:1343–8.
6. Hayabuchi Y, Sakata M, Ohnishi T, et al. A novel bilayer approach to ventricular septal deformation analysis by speckle tracking imaging in children with right ventricular overload. J Am Soc Echocardiogr. 2011;24:1205–12.
7. Hayabuchi Y, Sakata M, Kagami S. Assessment of the helical ventricular myocardial band using standard echocardiography. Echocardiography. 2014. doi:10.1111/echo.12624.
8. Di Salvo G, Russo MG, Paladini D, et al. Two-dimensional strain to assess regional left and right ventricular longitudinal function in 100 normal fetuses. Eur J Echocardiogr. 2008;9:754–6.
9. Schubert U, Müller M, Norman M, et al. Transition from fetal to neonatal life: changes in cardiac function assessed by speckle-tracking echocardiography. Early Hum Dev. 2013;89:803–8.
10. Jain A, Mohamed A, El-Khuffash A, et al. A comprehensive echocardiographic protocol for assessing neonatal right ventricular dimensions and function in the transitional period: normative data and Z scores. J Am Soc Echocardiogr. 2014;27:1293–304.
11. Levy PT, Holland MR, Sekarski TJ, et al. Feasibility and reproducibility of systolic right ventricular strain measurement by speckle-tracking echocardiography in premature infants. J Am Soc Echocardiogr. 2013;26:1201–13.
12. Singh GK, Cupps B, Pasque M, et al. Accuracy and reproducibility of strain by speckle tracking in pediatric subjects with normal heart and single ventricular physiology: a two-dimensional speckle-tracking echocardiography and magnetic resonance imaging correlative study. J Am Soc Echocardiogr. 2010;23:1143–52.
13. Friedman WF. The intrinsic physiologic properties of the developing heart. Prog Cardiovasc Dis. 1972;15:87–111.
14. Rudolph AM. Congenital diseases of the heart. Clinical-physiological considerations. 3rd ed. West Sussex: Wiley-Blackwell: 2009.
15. Rudski LG, Lai WW, Afilalo J, et al. Guidelines for the echocardiographic assessment of the right heart in adults: a report from the American Society of Echocardiography. Endorsed by the European Association of Echocardiography, a registered branch of the European Society of Cardiology, and the Canadian Society of Echocardiography. J Am Soc Echocardiogr. 2010;23:685–713.
16. Mertens L, Seri I, Marek J, et al. Targeted neonatal echocardiography in the neonatal intensive care unit: practice guidelines and recommendations for training. Writing group of the American Society of Echocardiography (ASE) in collaboration with the European Association of Echocardiography (EAE) and the Association for European Pediatric Cardiologists (AEPC). J Am Soc Echocardiogr. 2011;24:1057–78.
17. Koestenberger M, Ravekes W, Everett AD, et al. Right ventricular function in infants, children and adolescents: reference value of the tricuspid annular plane systolic excursion (TAPSE) in 640 healthy patients and calculation of z score values. J Am Soc Echocardiogr. 2009;22:715–9.
18. Kitabatake A, Inoue M, Asao M, et al. Noninvasive evaluation of pulmonary hypertension by a pulsed doppler technique. Circulation. 1983;68:302–9.
19. Mejia AAS, Simpson KE, Hildebolt CF, et al. Tissue Doppler septal Tei index indicates severity of illness in pediatric patients with congestive heart failure. Pediatr Cardiol. 2014;35:411–8.
20. Colan SD, Shirali G, Margossian R, et al. The ventricular volume variability study of the pediatric heart network: study design and impact of beat averaging and variable type on the reproducibility of echocardiographic measurements in children with chronic dilated cardiomyopathy. J Am Soc Echocardiogr. 2012;25:842–54.
21. Beyar R, Dong SJ, Smith ER, et al. Ventricular interaction and septal deformation: a model compared with experimental data. Am J Physiol. 1993;265:2044–56.
22. Evans N, Iyer P. Assessment of ductus arteriosus shunt in preterm infants supported by mechanical ventilation: effect of interatrial shunting. J Pediatr. 1994;125:778–85.
23. Haruki N, Takeuchi M, Kanazawa Y, et al. Continuous positive airway pressure ameliorates sleep-induced subclinical left ventricular systolic dysfunction: demonstration by two-dimensional speckle-tracking echocardiography. Eur J Echocardiogr. 2010;11:352–8.
24. Hammerstingl C, Schueler R, Wiesen M, et al. Impact of untreated obstructive sleep apnea on left and right ventricular myocardial function and effects of CPAP therapy. PLoS ONE. 2013. doi:10.1371/journal.pone.0076352.
25. Franchi F, Faltoni A, Cameli M, et al. Influence of positive end-expiratory pressure on myocardial strain assessed by speckle tracking echocardiography in mechanically ventilated patients. BioMed Res Int. 2013. doi:10.1155/2013/918548.
26. Fukuda Y, Tanaka H, Sugiyama D, et al. Utility of right ventricular free wall speckle-tracking strain for evaluation of right ventricular performance in patients with pulmonary hypertension. J Am Soc Echocardiogr. 2011;24:1101–8.
27. Giusca S, Dambrauskaite V, Scheurwegs C, et al. Deformation imaging describes right ventricular function better than longitudinal displacement of the tricuspid ring. Heart. 2010;96:281–8.
28. Torrent-Guasp F, Ballester M, Buckberg GD, et al. Spatial orientation of the ventricular muscle band: physiologic contribution and surgical implication. J Thorac Cardiovasc Surg. 2001;122:389–92.
29. Levy PT, Mejia AAS, Machefsky A, et al. Normal ranges of right ventricular systolic and diastolic strain measures in children: a systematic review and meta-analysis. J Am Soc Echocardiogr. 2014;27:549–60.
30. Takigiku K, Takeuchi M, Izumi C, et al. Normal range of left ventricular 2-dimensional strain: Japanese Ultrasound Speckle Tracking of the Left Ventricle (JUSTICE) study. Circ J. 2012;76:2623–32.

厚生労働科学研究費補助金　地域医療基盤開発推進研究事業

持続可能な広域医療情報連携ネットワークシステムの構築に関する研究
平成 27 年度　総括研究報告書

発行日　平成 28 年 3 月
発行者　岩手医科大学　小川　彰
〒020-8505　岩手県盛岡市内丸 19－1
TEL 019－651－5111（代）
発行所　　株式会社杜陵印刷